The Identification of Late Fields: A Multichannel High-Resolution State Space Approach

Martin Haardt, Peter Weismüller, and Reinmar Killmann

Abstract **— This paper presents a new multichannel parameter estimation approach based on low rank approximations of noisy block Hankel matrices. Different state space representations of the signals reveal the algebraic structure of the underlying model, resulting in a unified framework for dealing with uniformly spaced sensor arrays and the harmonic retrieval problem. Ultimately, these insights lead to improved parameter estimates. From the wide range of possible applications we will give a biomedical example: Late fields are identified from multichannel biomagnetic measurements.**

1. Introduction

Ventricular *late potentials* and ventricular *late fields* are low amplitude, high frequency oscillations that might occur at the end of and after the QRS complex of the heartbeat (Figure 1). They are identified in electrocardiographic (ECG) and magnetocardiographic (MCG) recordings, respectively, and represent slowed conduction in diseased myocardium, the muscular substance of the heart. Thus, they indicate deficiencies of the heart muscle, leading to an increased risk for developing ventricular arrhythmias [2]. Existing identification methods are based on periodograms, heuristic averaging and filtering techniques [1], [2]. Therefore, they neither allow a spatial localization nor a study of late fields in isolated heartbeats. This, however, can be achieved by *high-resolution* spectral estimation schemes that work with *multichannel* measurements of the heart activity.

The presented model-based approach assumes that all M sensor channels observe the same frequencies, where the amplitude and phase of a particular harmonic component can vary from channel to channel. *State space representations* expose the structure of this classical harmonic retrieval problem showing that exponentials can be generated by zero input oscillators in response to non zero initial conditions [6]. Since finite data records reveal only a poor approximation of covariance matrices, our approach does not use any variance-covariance information (as described in [4]), but works directly on the output of a given sensor array (*direct data approach*).

It will be shown that this new multichannel state space approach does not only solve the *harmonic retrieval* problem, but that it can also be used to estimate signal parameters, e.g., directions of arrival (DOAs), in narrow-band *array signal processing* using a uniform linear (equispaced) sensor array (ULA). Although the commonality between these data models is well known, their analysis has most of the time been treated separately. Therefore, a unified framework for the solution of these problems will be given in the next section. Furthermore, the new concepts presented in this paper can easily be extended to the time-varying case, as addressed in [5].

M. HAARDT was with Siemens AG, Corporate Research and Development, Munich, Germany. He is now with the Institute of Network Theory and Circuit Design, Technical University of Munich, Arcisstr. 21, D-80333 Munich, Germany.

P. WEISMÜLLER is with the Cardiology Department, University of Ulm, Ulm, Germany.

R. KILLMANN is with Siemens AG, Medical Engineering Group, Erlangen, Germany.

2. Data Model

The equivalence between the estimation of superimposed exponentials from multichannel measurements and the signal parameter estimation problem using a ULA will be established in this section.

2.1. Harmonic Retrieval

To this end, the harmonic retrieval problem is considered first: Let an (arbitrary) array of M sensors receive the sum of p (possibly damped) exponential signals. Then, $y_m(n)$, $1 \le m \le M$, the uncorrupted signal at sensor m, is given by

$$y_m(n) = \sum_{k=1}^{p} c_{k,m}\, \lambda_k^n, \qquad 0 \le n \le N-1, \tag{1}$$

where $c_{k,m}$ denotes the (complex) amplitude of the kth exponential observed from the mth sensor and $\lambda_k = |\lambda_k|\, e^{j\omega_k}$. After combining the observations at all M sensors to a signal vector $y(n) = [y_1(n), y_2(n), \ldots, y_M(n)]^T$, equation (1) can be expressed in a more compact form

$$y(n) = C^T\, \Lambda^n\, o, \tag{2}$$

where

$$C = \begin{bmatrix} c_{1,1} & c_{1,2} & \cdots & c_{1,M} \\ c_{2,1} & c_{2,2} & \cdots & c_{2,M} \\ \vdots & \vdots & \ddots & \vdots \\ c_{p,1} & c_{p,2} & \cdots & c_{p,M} \end{bmatrix}, \tag{3}$$

$\Lambda = diag(\lambda_1, \lambda_2, \ldots, \lambda_p)$, and $o = [1, 1, \ldots, 1]^T$. Throughout this paper, the transpose of a vector or a matrix A will be written A^T, and its conjugate transpose A^H, i.e., $A^H = \overline{A}^T$.

2.2. Uniform Linear Array

If, on the other hand, p narrow-band, possibly coherent, plane waves are incident on a ULA of N sensors, the mth snapshot is described by the output vector

$$z^T(m) = \left[\sum_{k=1}^{p} c_{k,m}, \sum_{k=1}^{p} c_{k,m} e^{j\omega_k}, \ldots, \sum_{k=1}^{p} c_{k,m} e^{j(N-1)\omega_k}\right], \tag{4}$$

where $\omega_k = (2\pi d/\lambda)\sin\theta_k$, d being the spacing between adjacent sensors, λ the associated carrier wavelength, and θ_k the DOA of the kth incident signal. Let M subsequent snapshots of the array output $z^T(m)$, $1 \le m \le M$, form the rows of an $M \times N$ matrix Y. This matrix can be expressed as

$$Y = C^T\, [o, \Lambda o, \ldots, \Lambda^{N-1} o]. \tag{5}$$

Notice, that the kth row of C contains M snapshots of the kth signal (3), while the second matrix in (5), representing the array characteristics, has a Vandermonde structure. Its p rows are known as steering or direction vectors and depend on the corresponding DOAs.

It is clearly seen from (2), that equation (5) also holds, if N subsequent data vectors $y(n), 0 \leq n \leq (N-1)$, taken from the harmonic retrieval problem, form the columns of Y. Consequently, both problems are equivalent, if

$$|\lambda_k| = 1 \qquad \forall\, k, \tag{6}$$

which is always satisfied in array processing applications with a ULA (4). In the harmonic retrieval problem, however, equation (6) obviously corresponds to the retrieval of undamped exponentials.

3. Multichannel State Space Approach

To extend the direct data approach presented in [6] to the multidimensional case, two multichannel state space descriptions of the harmonic oscillator are introduced.

Let $x(n)$ denote the state vector of dimension p (minimal system order). Then, the familiar *traditional state space model* is defined as:

$$\begin{array}{rcl} x(n+1) & = & F \quad x(n) \\ y(n) & = & H^T \quad x(n) \end{array} \tag{7}$$

Thus, we can express the current output vector $y(n)$ in terms of the state vector at time zero $x(0)$:

$$y(n) = H^T F^n x(0) \tag{8}$$

It is well known that a linear system has an infinite number of realizations, each of them having its own state space representation, characterized by the triple $\{F, H^T, x(0)\}$. All realizations can be obtained from one another through *similarity transformations*, i.e., by replacing $\{F, H^T, x(0)\}$ with $\{SFS^{-1}, H^T S^{-1}, Sx(0)\}$ for different choices of invertible $p \times p$ matrices S. One diagonal realization, for instance, is given by $\{\Lambda, C^T, o\}$.

The multichannel harmonic oscillator can also be described using the new *extended state description*, an alternative linear representation with matrix valued states $X(n) \in C^{\,p \times M}$:

$$\begin{array}{rcl} X(n+1) & = & F \quad X(n) \\ y^T(n) & = & h^T \quad X(n) \end{array} \tag{9}$$

Here, every sensor (harmonic retrieval) or snapshot (ULA) is represented by one of the M columns of $X(n)$ and equation (8) has the following counterpart:

$$y^T(n) = h^T F^n X(0) \tag{10}$$

Obviously, a particular realization is characterized by the triple $\{F, h^T, X(0)\}$. It is clear that all possible realizations can be obtained from $\{\Lambda, o^T, C\}$ using similarity transformations.

Although both models are equivalent, it will be shown that only the *extended state description* provides a possibility to further improve the estimation accuracy if equation (6) is satisfied (i.e., ULA or undamped exponentials). For notational convenience, the proposed algorithms will only be described in terms of the extended state description. Yet, it is fairly easy to apply all results to the traditional state space representation, unless otherwise indicated.

4. Estimation Procedure

4.1. Matrix Factorization

The presented algorithms are based on the factorization of block Hankel matrices $\tilde{B}$, constructed from noise-corrupted array measurements,

$$\tilde{y}(m) = y(m) + e, \tag{11}$$

where the noise vector e has dimension M.

In the noiseless case, the uncorrupted block Hankel matrix is defined as

$$B = \begin{bmatrix} y^T(0) & y^T(1) & \dots & y^T(N-L) \\ y^T(1) & y^T(2) & \dots & y^T(N-L+1) \\ \vdots & \vdots & \ddots & \vdots \\ y^T(L-1) & y^T(L) & \dots & y^T(N-1) \end{bmatrix}.$$

Using equation (10), it can be shown that B is rank-deficient, since it can be factored into a product of an $L \times p$ extended observability matrix Θ and a $p \times M(N-L+1)$ matrix Φ containing consecutive state vectors:

$$\begin{array}{rcl} B & = & \Theta \qquad\qquad\qquad\qquad \Phi \\ & = & \begin{bmatrix} h^T \\ h^T F \\ \vdots \\ h^T F^{L-1} \end{bmatrix} \begin{bmatrix} X(0), FX(0), \dots, F^{N-L} X(0) \end{bmatrix} \end{array} \tag{12}$$

4.2. Frequency or DOA Estimation

In the presence of additive noise, the block Hankel matrix $\tilde{B}$ has full rank with probability one. To obtain an optimum low rank approximation, the proposed algorithm starts by computing the singular value decomposition (SVD) of the noisy block Hankel matrix,

$$\tilde{B} = [U_1, U_2] \begin{bmatrix} \Sigma_1 & 0 \\ 0 & \Sigma_2 \end{bmatrix} \begin{bmatrix} V_1^H \\ V_2^H \end{bmatrix}, \tag{13}$$

where the diagonal matrix Σ_1 contains the p dominant singular values. The number of signals p is assumed to be either known or determinable via some information theoretical criteria, such as AIC of MDL [8]. After that, define $\hat{\Theta} = U_1\, \Sigma_1^{1/2}$ and $\hat{\Phi} = \Sigma_1^{1/2}\, V_1^H$. Obviously, $\hat{\Theta}\, \hat{\Phi}$ is the best rank p approximation of $\tilde{B}$ in the Frobenius norm [3].

$\hat{\Theta}$ deprived of its first and last row will be denoted by $\Theta\uparrow$ and $\Theta\downarrow$, respectively. In the noise-free case (12) we would have

$$\Theta\uparrow = \Theta\downarrow\, F. \tag{14}$$

With noisy measurements $\tilde{y}(m)$, however, there is no $p \times p$ feedback matrix F that exactly fulfills this overdetermined set of equations. A good approximation $\hat{F}$ can be found by solving (14) via *least squares* or *total least squares* [3].

Afterwards, an eigendecomposition of the estimated feedback matrix is performed, i.e.,

$$\hat{F} = S^{-1}\, \hat{\Lambda}\, S, \tag{15}$$

Note, that the the diagonal matrix $\hat{\Lambda}$, containing the eigenvalues of $\hat{F}$, approximates Λ. Therefore, the frequency estimates and damping factors (harmonic retrieval) or the DOAs (ULA) can be determined from $\hat{\Lambda}$.

4.3. Signal Reconstruction

In order to estimate the coefficient matrix C, notice also that S is a *similarity transformation* converting an extended state representation described by the triple $\{\hat{F}, h^T, X(0)\}$ into the diagonal realization $\{\hat{\Lambda}, h^T S^{-1}, SX(0)\}$. Motivated by these observations and equation (12), let us define

$$\hat{\Theta}\, S^{-1} = \begin{bmatrix} \theta_1^T \\ \theta_2^T \\ \vdots \\ \theta_L^T \end{bmatrix} \tag{16}$$

and

$$S\, \hat{\Phi} = \left[\phi_1, \phi_2, \ldots, \phi_{N-L+1}\right]. \tag{17}$$

These block matrices are multiplied by negative powers of $\hat{\Lambda}$ in the following fashion:

$$\begin{bmatrix} \theta_1^T & \\ \theta_2^T & \hat{\Lambda}^{-1} \\ \vdots & \vdots \\ \theta_L^T & \hat{\Lambda}^{-(L-1)} \end{bmatrix} \tag{18}$$

$$\left[\phi_1,\ \hat{\Lambda}^{-1}\phi_2,\ \ldots,\ \hat{\Lambda}^{-(N-L)}\phi_{N-L+1}\right]. \tag{19}$$

To eliminate the noise as much as possible, the arithmetic mean of the row vectors defined in equation (18) will be calculated. It is denoted by

$$\hat{h}^T = [h_1, h_2, \ldots, h_p].$$

Likewise, the arithmetic mean of the block matrices determined by (19) will be called $\hat{X}(0)$. Then, the proposed estimate of C can be determined in the following way:

$$\hat{C} = diag(h_1, h_2, \ldots, h_p)\ \hat{X}(0). \tag{20}$$

Due to the described *block averaging technique*, the resulting amplitude and phase estimates (harmonic retrieval) or signal estimates (ULA) are less noisy and, therefore, more accurate than those produced with the algorithm described in [6].

4.4. Estimation of Unitary Diagonal Matrices

As mentioned earlier, the new extended state description offers a convenient way of further improving the estimation accuracy in the case of undamped exponentials (harmonic retrieval) or array signal processing problems using a ULA. In both cases, equation (6) is satisfied and, consequently, Λ is a *unitary* diagonal matrix, i.e.,

$$\Lambda^{-1} = \Lambda^H = \overline{\Lambda}. \tag{21}$$

Using the diagonal extended state realization $\{\Lambda, o^T, C\}$ and equation (10) we get

$$\begin{aligned} y^T(n) &= o^T\ \Lambda^{n-(N-1)}\ \Lambda^{N-1}C \\ &= o^T\ \overline{\Lambda}^{(N-1)-n}\ X(N-1) \\ y^H(n) &= o^T\ \Lambda^{(N-1)-n}\ \overline{X}(N-1), \end{aligned}$$

yielding

$$y^H(n) = h^T\ F^{(N-1)-n}\ \overline{Z}(N-1) \tag{22}$$

via similarity transformations. Thus, the uncorrupted block Hankel matrix

$$B^b = \begin{bmatrix} y^H(N-1) & y^H(N-2) & \ldots & y^H(L-1) \\ y^H(N-2) & y^H(N-3) & \ldots & y^H(L-2) \\ \vdots & \vdots & \ddots & \vdots \\ y^H(N-L) & y^H(N-L-1) & \ldots & y^H(0) \end{bmatrix}$$

can be factorized into $\Theta\, \Phi^b$ with

$$\Phi^b = \left[\overline{Z}(N-1), F\overline{Z}(N-1), \ldots, F^{N-L}\overline{Z}(N-1)\right]$$

such that $y^H(N-1) = h^T\overline{Z}(N-1)$. Combining this with previous results (12), we can factorize a concatenation of two block Hankel matrices

$$B^{fb} = \left[\, B,\ B^b \,\right] = \Theta\, \left[\, \Phi,\ \Phi^b \,\right]. \tag{23}$$

Replacing $\tilde{B}$ by $\tilde{B}^{fb}$, the noise corrupted version of B^{fb}, in the algorithm described above, will, therefore, yield a unitary diagonal feedback matrix $\hat{\Lambda}$. Simulations have shown that this *forward-backward estimation technique* improves the frequency or DOA estimates significantly.

5. Identification of Late Fields in MCG Recordings

Our proposed method for the identification of late fields or late potentials in MCG or ECG recordings consists of three steps: First, the algorithm identifies (triggers) the maximum of the QRS-complex and extracts the relevant data from all M channels (Figure 1). Then, a constant offset and a linear trend are compensated via least squares. This compensation is performed in all M channels independently. Finally, the presented multichannel spectral estimation scheme determines the frequencies of the superimposed harmonics using the *traditional* or the new *extended state description* (harmonic retrieval). Notice that the described algorithm can also estimate the complex amplitudes of the dominant harmonic components in the individual channels (1), which will help clinicians to determine the spatial position of the heart deficiencies.

Experiments with data, recorded by a biomagnetic multichannel sensor system (KRENIKON^{R}) [7], show promising results. The frequencies found using the *extended state representation* were plotted as histograms. While Figures 2 and 3 show histograms of patients with late fields, Figures 4 and 5 depict those of healthy individuals. All four histograms have two peaks in the low frequency range around 15 Hz and 50 Hz. They are caused by the final portion of the QRS-complex (Figure 1) and the European net frequency, respectively. Nevertheless, the histograms differ at high frequencies. While histograms of patients with late fields are characterized by a significant amount of harmonics in the high frequency range (around 200 Hz), those of healthy individuals do not exhibit this phenomena. Therefore, late fields can apparently be diagnosed by plotting histograms of the estimated frequencies. These first results, that seem to be superior to existing identification schemes [1], [2], still have to be confirmed by a systematic clinical evaluation.

6. Acknowledgment

The first author would like to thank Peter Strobach for many valuable discussions and for pointing out the fact that no method of recording and analyzing late fields in routine examinations has been established.

7. References

[1] D.E. Balderson, D.W.G. Harron, O. Escalona, and R.H. Mitchel. "The detection, significance and effect of drugs upon ventricular late potentials". *Automedica*, vol. 13, pp. 67-96, 1991.

[2] E.J. Berbari and R. Lazzara. "An Introduction to High-Resolution ECG Recordings of Cardiac Late Potentials". *Arch. Intern. Med.*, vol. 148, pp. 1859-1863, August 1988.

[3] G.H. Golub and C.F. van Loan. *Matrix Computations*. Johns Hopkins University Press, Baltimore, MD, 2nd edition, 1989.

[4] S.Y. Kung, K.S. Arun, and D.V. Bhaskar Rao. "State space and SVD based approximation methods for the harmonic retrieval problem". *J. Opt. Soc. Amer.*, vol. 73, pp. 1788-1811, December 1983.

[5] M.W.Y. Poon, R.H. Khan, and S. Le-Ngoc. "A Singular Value Decomposition (SVD) Based Method for Suppressing Ocean Clutter in High Frequency Radar". *IEEE Trans. Signal Processing*, vol. 41, pp. 1421-1425, March 1993.

[6] Bhaskar D. Rao and K.S. Arun. "Model Based Processing of Signals: A State Space Approach". *Proc. IEEE*, vol. 80, pp. 283-309, February 1992.

[7] S. Schneider, E. Hoenig, H. Reichenberger, K. Abraham-Fuchs, G. Daalmans, W. Moshage, A. Oppelt, G. Röhrlein, H. Stefan, J. Vieth, A. Weikl, and A. Wirth. "Multichannel biomagnetic system for high-resolution functional studies of brain and heart". *Radiology*, vol. 176, pp. 825-830, 1990.

[8] M. Wax and T. Kailath. "Detection of Signals by Information Theoretic Criteria". *IEEE Trans. Acoust., Speech, Signal Processing*, vol. ASSP-33, pp. 387-392, April 1985.

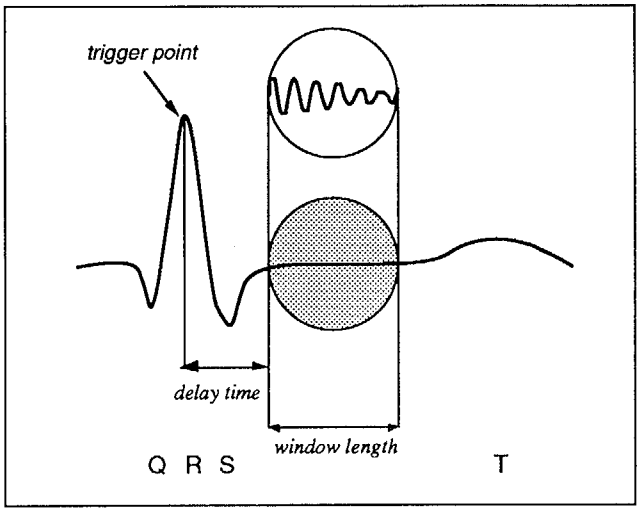

Fig. 1: Ventricular late fields

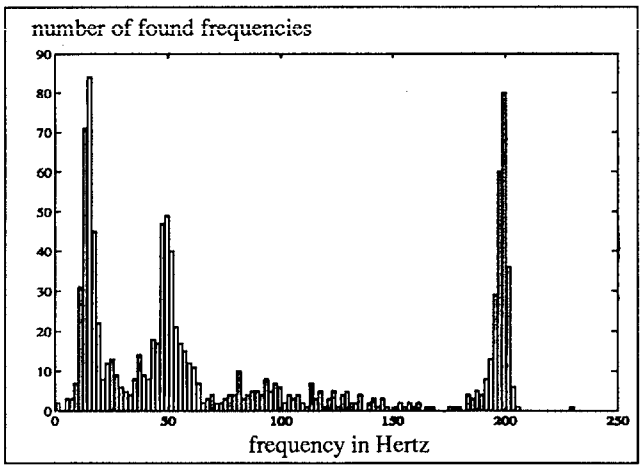

Fig. 2: Patient with late fields: 344 heartbeats, 1032 frequencies

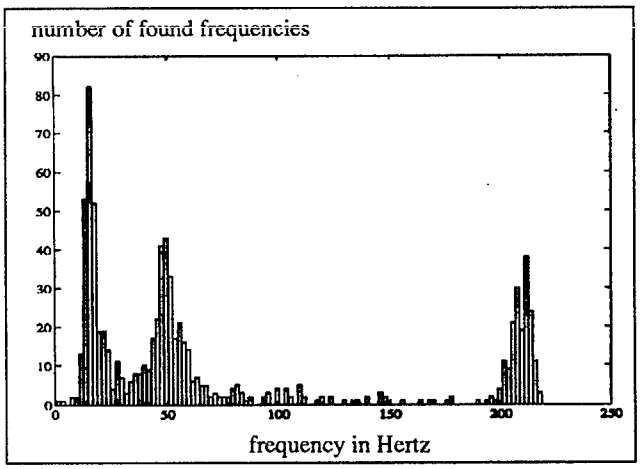

Fig. 3: Patient with late fields: 288 heartbeats, 817 frequencies

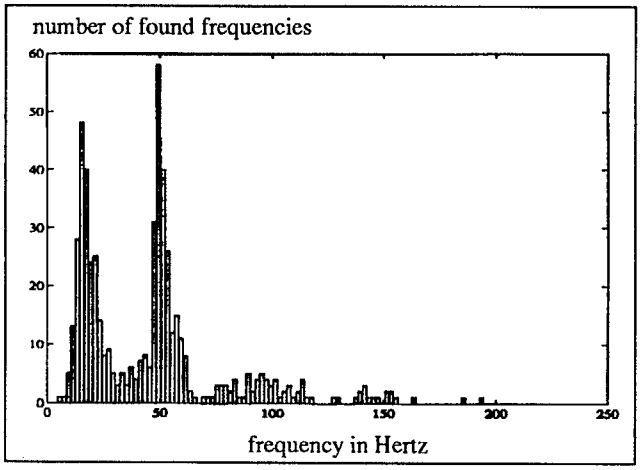

Fig. 4: Patient without late fields: 239 heartbeats, 548 frequencies

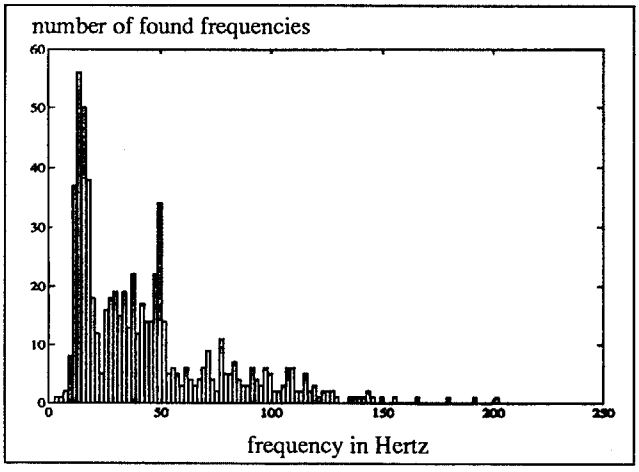

Fig. 5: Patient without late fields: 243 heartbeats, 650 frequencies